PROCESSING OF FLUORAPATITE FILMS WITH DIFFERENT THICKNESS ON POROUS ZIRCONIA TAPES

María P. Albano, Liliana B. Garrido
Centro de Tecnología de Recursos Minerales y Cerámica (CETMIC), C.C.49 (B1897ZCA) M. B. Gonnet, Provincia de Buenos Aires, ARGENTINA.
E-mail:palbano@cetmic.unlp.edu.ar

ABSTRACT

Fluorapatite (FA) layers with different thickness on porous 3 mol% yttria-partially stabilized zirconia (Y-PSZ) substrates have been fabricated by dipping porous zirconia tapes into aqueous fluorapatite slurries. Two different binders,poly(vinyl)alcohol (PVA) and latex were used to prepare the fluorapatite dip coating slips. The influence of the suspension properties and the porous structure of the tape surfaces (top and bottom) on the formation rate and consequently on the layer thickness formed on each surface were studied. A greater initial thickness of the layer adhered was found for the tapes dip coated in the FA slip with latex; for immersion times>0, the casting rate at the top surface of the tapes was greater than that at the bottom surface for both dip-coating slips. The higher casting rate of the slips with latex produced layers with thickness 8-9 times greater on both tape surfaces relative to the slip prepared with PVA.

Keywords: Porous ZrO_2 tapes; fluorapatite layers; dip coating

INTRODUCTION

Calcium orthophosphates such as fluorapatite ($Ca_{10}(PO_4)_6F_2$) are widely used as bone substitute materials due to their chemical similarity to the mineral component of mammalian bones and theeth (1). Fluorapatite is non-toxic, biocompatible, exhibits bioactive behaviour and integrates into living tissue by the same processes active in

remodelling healthy bone. These characteristics lead to an intimate physicochemical bond between the implants and bone, termed osteointegration. Even so, the major limitations to use fluorapatite as load-bearing biomaterials is its mechanical properties, it is brittle with a poor fatigue resistance . The poor mechanical behaviour is even more evident for highly porous ceramics and scaffolds ; that is why, in biomedical applications fluorapatite is used primarily as fillers and coatings. Bioinert ceramic such as porous ZrO_2 can be coated with FA to achieve a high mechanical strength as well as a suitable biocompatibility of the system (2).

The coating layer produced by the plasma- spraying technique is thick (~50-200 µm) and relatively dense; however, phase instability and non-uniformity are some of its weaknesses . The films synthesized by sol-gel and physical vapor deposition methods are too thin (~1 µm) to be applied for long-term usage. Coating layers dense and uniform with thickness of 5-20 µm retaining high chemical and thermal stability can be produced by dip coating.

We have previously studied the tape casting process to produce porous zirconia substrates using starch and an acrylic latex emulsion as fugitive additive and binder, respectively (3). Besides, the processing of stable concentrated aqueous FA suspensions with the addition of ammonium polyacrylate (NH_4PA) and Poly(vinyl)alcohol (PVA) as dispersant and binder, respectively, was investigated (4). In this work, porous Y-PSZ tapes with 31.4 vol.% porosity were produced by tape casting and characterized with specific attention directed to the microstructure of the top and bottom surfaces of the sintered tapes. Then, sections of these tapes were dip coated into the different concentrated aqueous FA slurries to produce FA layers.

Two mechanisms govern the formation of a layer on a porous body during dip coating. The first mechanism is known as liquid entrainment, and occurs as the plate-like specimen is withdrawn from the slurry faster than the liquid can drain from its surface, leaving a thin slurry film (5). The second mechanism is slip casting, the capillary suction caused by the porous substrate drives ceramic particles to concentrate at the substrate-suspension boundary, and a wet layer is formed (6). The withdrawal velocity of the specimen and the suspension viscosity have influence on the liquid entrainment mechanism. The microstructure of the substrate (porosity and pore diameter) together with the structure of the wet layer have influence on the slip casting mechanism. In this work, two different binders PVA and an acrylic latex emulsion were used to prepare the FA suspensions. The influence of the suspension

properties and the porous structure of the tape surfaces (top and bottom) on the formation rate and consequently on the layer thickness formed on each surface were studied. Layers formed on the top and bottom surfaces of the tapes by using the different dip-coating slips and their respectively microstructure were compared.

EXPERIMENTAL PROCEDURE

Raw materials and processing

A commercial 3 mol% yttria- partially stabilized zirconia doped with 0.3 wt% Al_2O_3 (Saint-Gobain ZirPro, Chine) was used to produce the cast tapes. The mean particle diameter and the specific surface area were 0.15 μm and 12.25 m^2/g, respectively. Potato starch with a median equivalent diameter of about 50 μm was used as pore former agent.

A commercial ammonium polyacrylate (NH_4PA) solution (Duramax D 3500, Rohm & Haas, Philadelphia PA) was used as a dispersant. The binder was an acrylic latex emulsion (Duramax B1000, Rohm & Haas, Philadelphia PA) with solids loading of 55 wt. %, an average particle size of 0.37 μm.

The $Ca_3(PO_4)_2$ (Fluka, Germany) and CaF_2 (Sigma–Aldrich, Ireland) powders were mixed in stoichiometric ratio and calcined 3 hs at 1000 °C. Then, the powder was milled in an attrition mill using 1.6 mm zirconia balls with 0.047 wt% NH_4PA during 48 hours. The milled powder was washed with distilled water and dried at 100 °C. This powder subsequently referred as FA was used to prepare the suspensions for dip coating. NH_4PA was used as deflocculant and two different binders a 9 wt% PVA solution and the acrylic latex emulsion were employed to prepare the different FA suspensions.

Concentrated aqueous Y-PSZ suspensions with a solid loading of 77 wt. % were prepared by deagglomeration of the powder in distilled water with 0.3 wt.% NH_4PA (dry weight base of powder) using an ultrasonic bath. 13 wt% of starch (dry weight base of Y-PSZ powder) was added to the stabilized Y-PSZ slips followed by ultrasonic treatment. Subsequent to this, 25 wt. % latex (dry weight basis with respect to (Y-PSZ + starch) powders) was added to the slurry, followed by additional stirring. The pH of the suspensions was adjusted to 9.0 with ammonia (25 wt. %).

The Y-PSZ slips were cast manually on a Mylar film using an extensor. The gap between the extensor and the film was adjusted to 0.4 mm. The cast tapes were subsequently dried in air at room temperature up to constant weight; afterwards, they were stripped from the film and sectioned into rectangular pieces of 2.75 cm x 1.65 cm. The burn out of organic additives was achieved by slow heating (1 °C/min) up to 1000 °C. Then, the pre-calcined tapes were sintered at 1500 °C for 2 h, with a heating rate of 5 °C/min.

Aqueous FA slips with 0.6 wt% NH_4PA and different contents of the two binders: 5 wt% PVA and 15 wt% latex, were prepared by suspending particles in deionized water via 20 min of ultrasound; the pH was manually adjusted to be maintained at 9. The sintered tapes were vertically dipped into the FA suspension; after immersion during different times they were withdrawn from the suspension at a constant rate of 8 mm/s. The dip-coated samples were allowed to dry at room temperature in the vertical orientation, further dried in air at 60 °C, heated for 30 min at 600 °C for binder burn out and sintered at 1200 °C for 1h.

Characterization techniques

The microstructure of sintered samples were observed on both the top side of the tape (exposed to air during casting/drying), and the bottom side (exposed to the carrier surface during casting/drying) using a scanning electron microscopy (SEM) (JEOL, JSM-6360).

The viscosity of the aqueous FA slips with 0.6 wt% NH_4PA and different contents of the two binders: 5 wt% PVA and 15 wt% latex were measured. Steady state flow curves of FA slips were performed by measuring the steady shear stress value as a function of shear rate in the range of 0.5 to 542 s^{-1} using a concentric cylinder viscometer (Haake VT550, Germany) at 25 °C.

Dipped tapes were diamond polished and examined by SEM; the layer thickness on the top and bottom surfaces was measured. The microstructure of the FA coating layer after sintering produced using the different dip coating slips was observed by SEM.

RESULTS AND DISCUSSION

Two mechanisms govern the formation of a layer on a porous body during dip coating. The first mechanism is known as liquid entrainment, and ocurrs as the plate-like specimen is withdrawn from the slurry faster than the liquid can drain from its surface, leaving a thin slurry film (5). This film thickness, h, is given by:

$$h=0.94\ (\gamma/\delta\ g)^{1/2}\ Ca^{2/3} \qquad (A)$$

Ca is the capillary number given by (18):

$$Ca=\eta\ V/\gamma \qquad (B)$$

where γ is the surface tension, δ is the slurry density, g is the gravity acceleration, η is the slurry viscosity and V is the withdrawal velocity. As the liquid from the thin layer of slurry evaporates, a thin coating of ceramic particles remains on the surface of the specimen. The second mechanism is a slip-casting phenomenon and occurs because the tapes, when dipped, are slightly porous and dry. The capillary suction caused by the porous substrate drives ceramic particles to concentrate at the substrate-suspension boundary, and a wet membrane, or cake, is formed, as in the slip casting process (6). In this capillary filtration, the driving force is the capillary suction pressure caused by all the pores on the surface of the substrate. Fluid flow through the consolidated layer and into the porous body is governed by Darcy′s law, which can be integrated and simplified (assuming that the permeability of the substrate is much larger than that of the layer) to express the thickness of the sintered layer,L, as a function of time, t, in the form (6):

$$L=2\ (\ \varepsilon_s\ \gamma\ k_m\ t/\mu\ \alpha\ R)^{1/2} \qquad (C)$$

Where ε_s is the porosity of the substrate, k_m is the permeability of the wet layer, t is the time, R is the pores radius and μ represents the dispersion liquid viscosity; α is defined as:

$$\alpha=(\ \varphi_0\ /\ \varphi_m)\ -\ 1 \qquad (D)$$

where φ_0 and φ_m are the volume fraction of the particles in the suspension and in the wet layer, respectively. During the subsequent drying and sintering process, the layer shrinks only in the direction perpendicular to the substrate, the thickness of the sintered layer, $L_{sintered}$, can be expressed as (6):

$$L_{sintered}=\beta\ L \qquad (E)$$

Where β is defined as:

$$\beta=\varphi_m\ /\ (1-\varepsilon_m) \qquad (F)$$

ε_m is the porosity of the sintered layer. Substituting eq (C) and (F) into eq (E) gives:

$$L_{sintered} = 2\varphi_m / (1- \varepsilon_m) (\varepsilon_s \gamma k_m t/\mu \alpha R)^{1/2} \quad (G)$$

Figure 1 shows the layer thickness after sintering versus immersion time for the top and bottom surfaces of the tapes dip coated in the different FA suspensions. The layer thickness squared versus immersion time for the tapes dip coated in the FA slurries prepared with PVA and latex are shown in Figs. 2a and 2b, respectively.

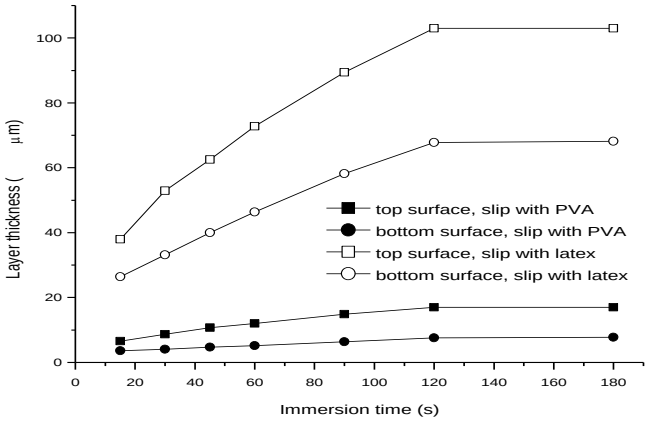

Figure 1: Layer thickness after sintering versus immersion time for the top and bottom surfaces of the tapes dip coated in the different FA suspensions.

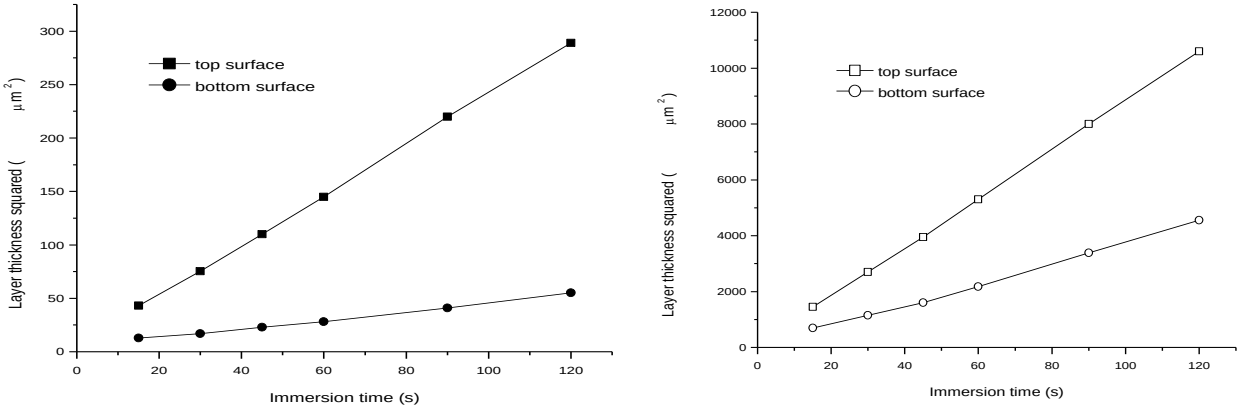

a b

Figure 2: Layer thickness squared versus immersion time for the tapes dip coated in the FA slurries prepared with the different binders: (a) PVA; (b) latex.

Figure 3a and 3b show the flow curves of shear stress versus shear rate and viscosity versus shear rate, respectively, at pH 9 for the different FA slips.

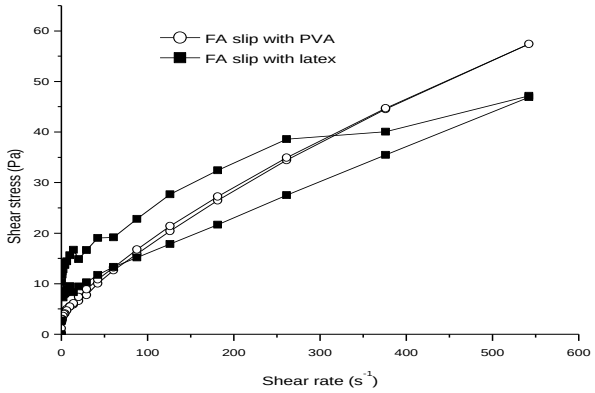

a

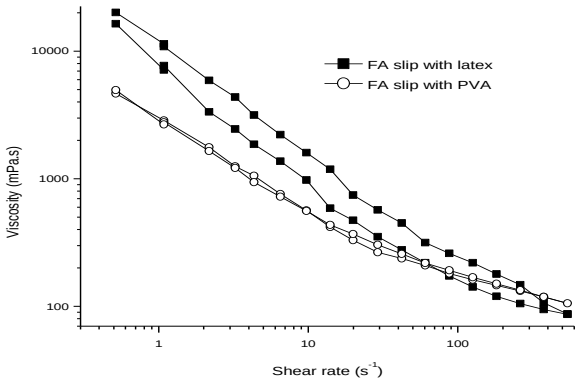

b

Figure 3: (a) Flow curves of shear stress versus shear rate and (b) viscosity versus shear rate, at pH 9 for the different FA slips.

The measured flow curves were satisfactorily fitted with the Casson model (R=0.99). The Casson model equation is:

$$\tau^{1/2} = \tau_0^{1/2} + (\eta_p \gamma)^{1/2} \qquad (H)$$

where τ is the shear stress, γ is the shear rate, τ_0 is the yield stress and η_p represents the limiting viscosity at a high shear rate range. The particles in a flocculated suspension form floc groups or a network, because of the mutual attraction between particles, and the yield stress value of the Casson model could be used as a parameter that indicated the degree of aggregation and consequently the degree of slip flocculation. The η_p value becomes equal to the viscosity when $\tau_0 \rightarrow 0$. Table 1 shows the composition and rheological parameters of the different FA slips.

Table1: Composition and rheological parameters of the different FA slips.

FA slips	Volume fraction of solids (%)	τ_0 (Pa)	η_p(Pa.s)
with PVA	27.4	1.86	0.076
with latex	36.2	7.62	0.052

In the regime of low shear rates as proceeds in the dip coating process (5), higher shear stress and viscosity values were found for the FA slips prepared with latex with respect to those for the slips with PVA. The slips exhibited a pseudoplastic behaviour and the slips prepared with latex show a strong shear thinning tendency. The low τ_0 value of the slip prepared with PVA indicated a weakly flocculation; while the slip with latex was strongly flocculated with an attractive network (high τ_0 value, table 1). The higher resistance to flow of the slip with latex avoided any settling of the particles by reducing their mobility.

The lines in Figs. 2a and 2b did not pass through the origin instead they intersected the y- vertical axis at a thickness value of about 13 and 3 μm for the slips prepared with latex and PVA, respectively. As we have previously mentioned the first mechanism in the layer formation was the liquid entrainment which leaved a thin slurry film on the tape surface eq. (A). As the viscosity values at low shear rates of the slips with latex were four times higher than those of the slips with PVA, a greater thickness of the film adhered, h, could be expected. As the data for the different slips were obtained by using identical withdrawal velocity, the greater thickness of the layer produced using the slip with latex at the initial stage was attributed to the higher viscosity of the slip with latex and its effect on the liquid entrainment mechanism eqs. (A) and (B).

The equation (C) shows that when the suspension and substrate are fixed, the layer thickness squared increases linearly with the dipping time. A linear relation between the thickness squared and the dipping time up to 120 s was found (Figs. 2a and 2b), suggesting that these data were in good agreement with the eq. (C) for the casting mechanism. For immersion times>0, the casting rate was observed to be strongly influenced by both the structure of the tape surfaces and the suspension properties. In a previous paper, the authors characterized the top and bottom surfaces of the tapes with a total bulk porosity of 31.4 vol.% (7). Fig. 4 shows micrographs of the top and bottom surfaces of the sintered tape.

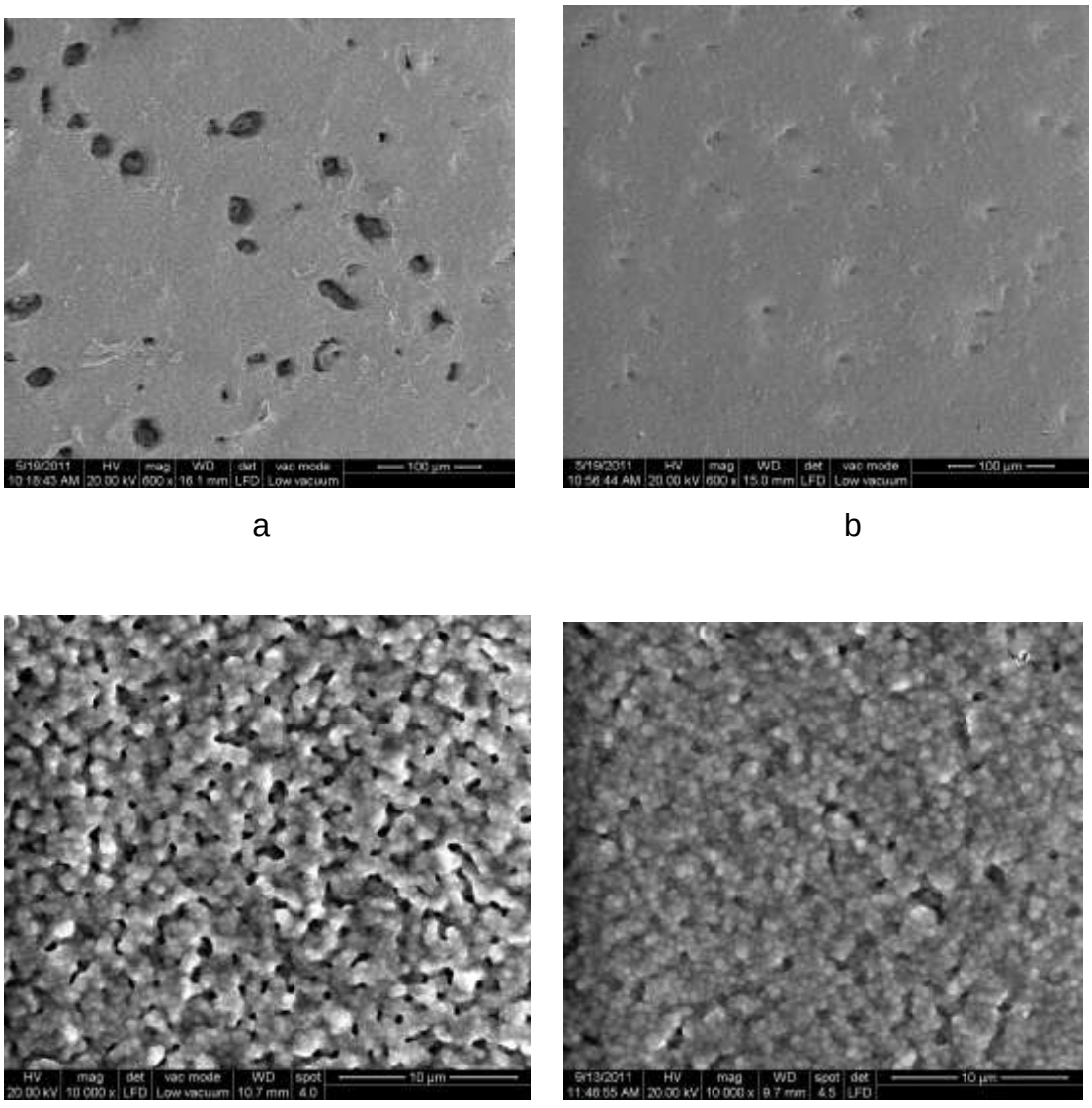

a b

c d

Figure 4: SEM micrographs of the surfaces of a sintered tape: (a) top surface; (b) bottom surface; (c) top surface matrix; (d) bottom surface matrix.

As we have mentioned the top surface was exposed to air during casting/drying while the bottom one was in contact with the film carrier. The surfaces were different; a greater number of large pores created by the starch particles (lengths between 15 and 80 μm) (Figs. 4a and 4b) and also a greater number of smaller pores in the matrix (lengths between 0.6 and 3.0 μm) (Figs. 4c and 4d) were found on the top surface with respect to those on the bottom one. The starch particles migrated to the top surface during casting due to its lower density (1.45 g/cm^3) in comparison with 6.05 g/cm^3 for Y-PSZ. In addition, the latex particle clusters migrated in the same direction as the solvent, to the top surface, as drying proceeded (7). Thus, the

migration of the starch and the consolidated latex particles to the top surface during casting and drying, respectively, resulted in an increase in porosity of the top surface after sintering relative to that of the bottom surface. The greater porosity and the larger number of smaller pores increased the casting rate eq. (C) of the top surface producing thicker dip coated layers.

The FA slip prepared with latex produced layers with thickness 8-9 times greater on both tape surfaces relative to the slip prepared with PVA (Fig. 1). Thus, the casting rate of the slip with latex was greater with respect to that with PVA, resulting in an increase of the layer thickness. As it was mentioned, the layer formation process by dip coating is similar to the formation of a cake on a porous mould by slip casting (6)' in both the driving force for the liquid flow is the capillary suction pressure of the substrate. We have previously studied the casting rate of FA suspensions with different viscosities and the resultant green cake microstructure (8). Our results demonstrated that the volume and size of the most frequent pore radius within the cake increased when the slip with high viscosity was cast. The greater porosity and pore size increased the permeability of the cake (k_m), thereby increasing the casting rate eq. (C). In the slips with lower viscosity values the particles could pack in an ordered way due to the repulsive forces existing between them, resulting in a lower permeability of slip cast bodies (8). In this work, a greater permeability of the wet layer produced with the FA slip prepared with latex (high viscosity values) and consequently a greater casting rate could be expected eq. (C).

Figure 5 shows the microstructure of the FA coating layer after sintering produced using the different dip coating slips. A greater porosity and pore size of the FA sintered layer was found when the dip coating slurry was prepared with latex. The FA sintered layer produced using the dip coating slurry with latex had rounded and elongated pores with lengths between 0.8 and 4.0 µm; while the layer formed using the slip with PVA had small pores with lengths between 0.4 and 2.3 µm. For the layer produced using the slip with latex, the coalescence of the latex particles during drying and the pore coalescence during sintering might contribute to the enlargement of the pores in the layer.

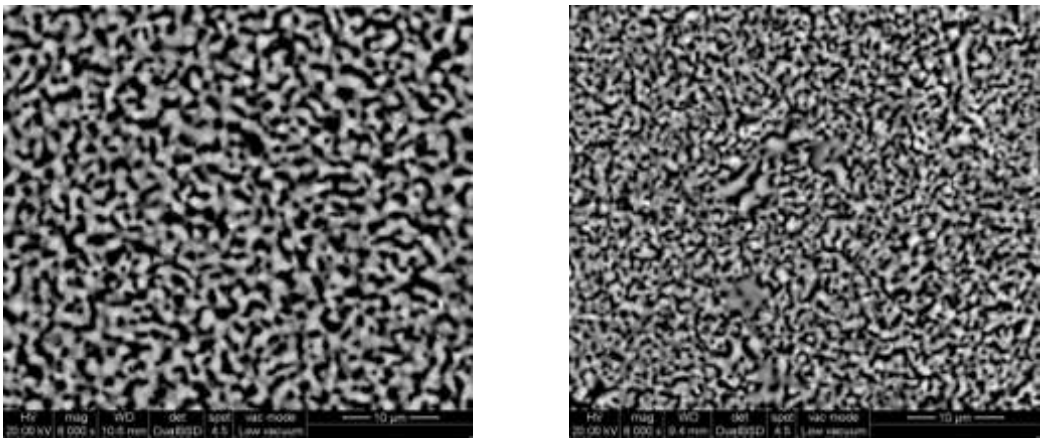

a b

Figure 5: Microstructure of the FA coating layer after sintering produced using the different dip coating slips: (a) with latex; (b) with PVA.

The onset of the latex coalescence is expected to occur during the drying of the layer when the volume fraction of latex particles approaches 0.6, its maximum solids loading (9). The latex coalescence resulted in an increase in the particle size of the latex, thereby increasing the pore size left by the latex during burnout. The pores could also coalesce during sintering so that the pore size increased; the enlargement of the pores leads to a decreased sintering rate. Therefore, the large pores in the layer reduced the sinterability of FA leading to a greater porosity and pore size in the sintered layer. The greater porosity of the sintered layer (ε_m) increased its thickness, $L_{sintered}$, by increasing β eqs. (E) and (F). Thus, the greater thickness of the sintered layer formed using the slip with latex for immersion times > 0 was attributed to the greater permeability of the wet layer which increased the casting rate eq. (C), together with the higher volume fraction of particles in the slip and the more porous layer structure produced by the presence of latex eq. (G). The liquid entrainment mechanism at the initial stage and slip casting for longer immersion times were both accelerated by using the dip coating slip with latex.

CONCLUSIONS

Fluorapatite layers with different thickness on porous Y-PSZ substrates have been fabricated by dipping porous zirconia tapes into aqueous fluorapatite slurries. Two different binders, PVA and latex were used to prepare the fluorapatite dip coating slips. The formation of a layer on the surface of the tapes was governed by liquid entrainment at the initial stage and slip casting for longer immersion times; both

mechanisms were accelerated by using the dip coating slip with latex. A greater initial thickness of the layer adhered was found for the tapes dip coated in the FA slip with latex due to the higher viscosity of the slip and its effect on the liquid entrainment mechanism. For immersion times>0, the casting rate was observed to be strongly influenced by both the structure of the tape surfaces and the suspension properties. For both FA slurries, the casting rate at the top surface of the tapes was greater than that at the bottom surface. The higher casting rate of the slips with latex produced layers with thickness 8-9 times greater on both tape surfaces relative to the slip prepared with PVA.

REFERENCES

(1) Weiner, S.; Wagner, H. D. The material bone: structure- mechanical function relations. Ann. Rev. Mater. Sci., v. 28, p. 271-298, 1998.

(2) Kim, H.-W.; Lee, S.- Y.; Bae, C.-J.; Noh, Y.-J.; Ko, J. S. Porous ZrO_2 bone scaffold coated with hydroxyapatite with fluorapatite intermediate layer. Biomaterials, v. 24, p. 3277-3284, 2003.

(3) Albano, M. P.; Genova, L.; Garrido, L. B.; Plucknett, K. Processing of porous yttria-stabilized zirconia by tape-casting. Ceramics International, v. 34, p. 1983-1988, 2008.

(4) Albano, M. P.; Garrido, L. B. Processing of concentrated aqueous fluorapatite suspensions by slip casting. Journal of Materials Science, v. 46, p. 5117-5128, 2011.

(5) Pontin, M. G.; Lange, F. F.; Sánchez-Herencia, A. J.; Moreno, R. Effect of unfired tape porosity on surface film formation by dip coatin., J. Am. Ceram. Soc.,v. 88, n.10, p. 2945-2948, 2005.

(6) Gu, Y. and G. Meng, A model for ceramic membrane formation by dip-coating. J. Eur. Ceram. Soc., v. 19, p. 1961-1966, 1999.

(7) Albano, M. P.; Garrido, L. B. Effect of zirconia tape porosity on fluorapatite film formation by dip coating. Ceramics International, En prensa, 2013 .

(8) Albano, M. P.; Garrido, L. B. Processing of concentrated aqueous fluorapatite suspensions by slip casting. J. Mater. Sci., v. 46, n. 15, p. 5117-5128, 2011.

(9) Smay. J. E.; Lewis. J. A. Structural and property evolution of aqueous-based lead zirconate titanate tape-cast layers. J. Am. Ceram. Soc, v. 84, n. 11, p. 2495-2500, 2001.